Supplementary data

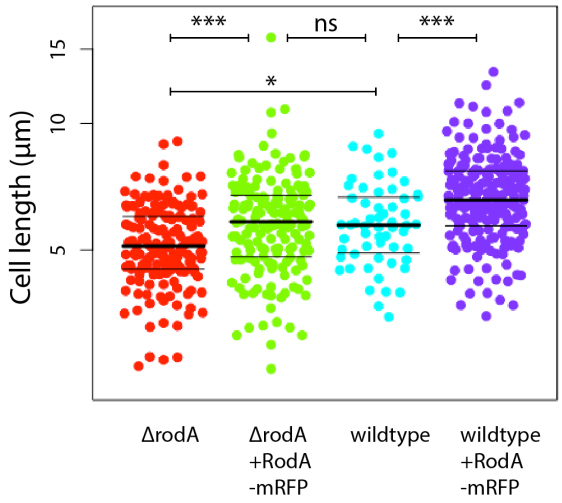

Figure S1: RodA-mRFP fusion complements Δ*rodA*. Phase images of ΔrodA + empty vector, ΔrodA + *rodA-mRFP*, wildtype + empty vector, and wildtype + *rodA-mRFP* were acquired and cell lengths were quantified using Oufti, MATLAB (1), and visualized using R Studio (58<n<204). Significance determined using analysis of variance (ANOVA) followed by a Tukey post hoc test to conduct pairwise comparisons. ns, not significant; *, p<0.05; **, p<0.01; ***, p<0.005.

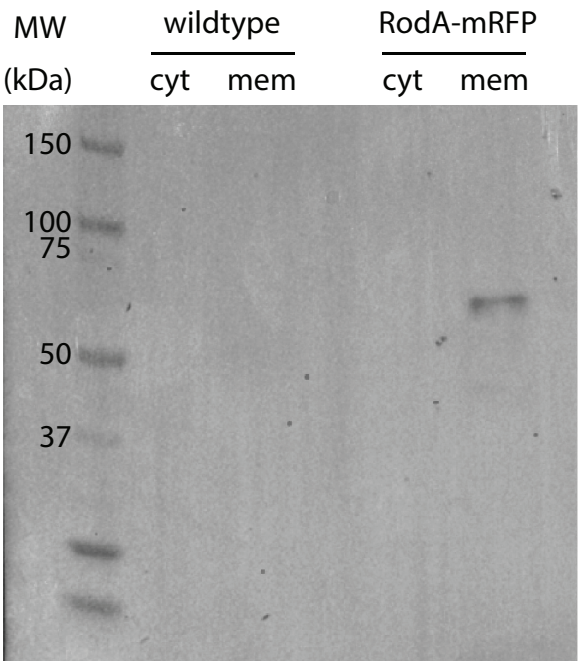

Figure S2: RodA-mRFP fusion localizes to the plasma membrane with minimal degradation. Lysates from *M. smegmatis* +/- *rodA-mRFP* were separated into cytoplasmic (cyt) and membrane (mem) fractions by ultracentrifugation and immunoblotted with anti-RFP antibodies. Protein concentration normalized.

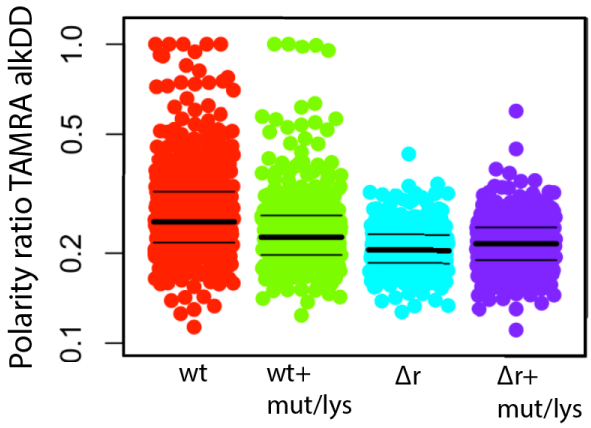

Figure S3: Polarity of cell wall synthesis detected with TAMRA. Polarity ratio of cell wall labeling (bright pole signal/total cell fluorescence) in wildtype and Δ*rodA* +/- mutanolysin/lysozyme. Nascent peptidoglycan labeled as in Fig. 2a except that click chemistry detection was with picolyl azide-TAMRA.

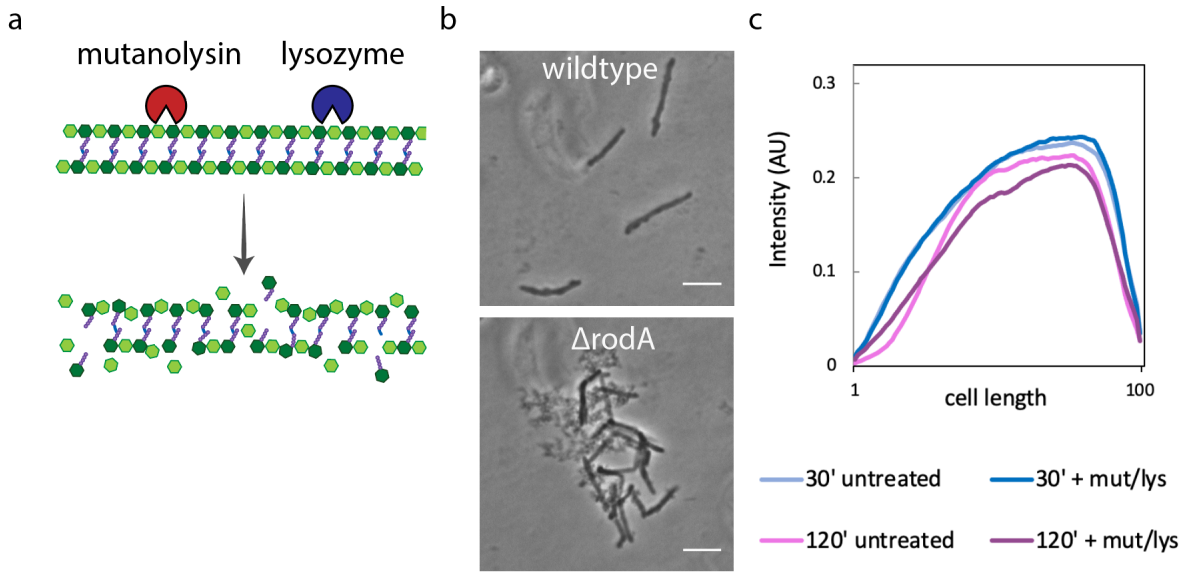

Figure S4: Mutanolysin/lysozyme treatment leads to cell-wide damage. (a) Muramidases mutanolysin and lysozyme break the linkages between neighbouring glycans *N*-acetylglucosamine and *N*-acetylmuramic acid in the peptidoglycan backbone (b) Phase contrast images of wildtype or Δ*rodA M. smegmatis* +/- mutanolysin/lysozyme. Scale bars = 5 μm. (c) *M. smegmatis* was labeled with 1μM RADA, a D-amino acid monopeptide that we previously showed incorporates into peptidoglycan via L,D-transpeptidases (2) and coats the cell wall evenly after overnight incubation with a low concentration (3). After washing, the culture was treated with

mutanolysin/lysozyme and loss of fluorescence along the length of the cells was quantitated. As expected, after 2 hours labeling loss was observed at the poles in untreated cells. Loss of fluorescence at the poles of lysozyme/mutanolysin-treated *M. smegmatis* was not as pronounced, consistent with its slow growth in the presence of the enzymes (Figure 5a). At this time point, sidewall loss of fluorescence was greatly enhanced with enzyme treatment. Although mycobacterial growth precludes interpretation of cell wall loss at the poles, these data suggest that lysozyme/mutanolysin-mediated cell wall loss occurs along the *M. smegmatis* sidewall. Signal not normalized. 58<n<102.

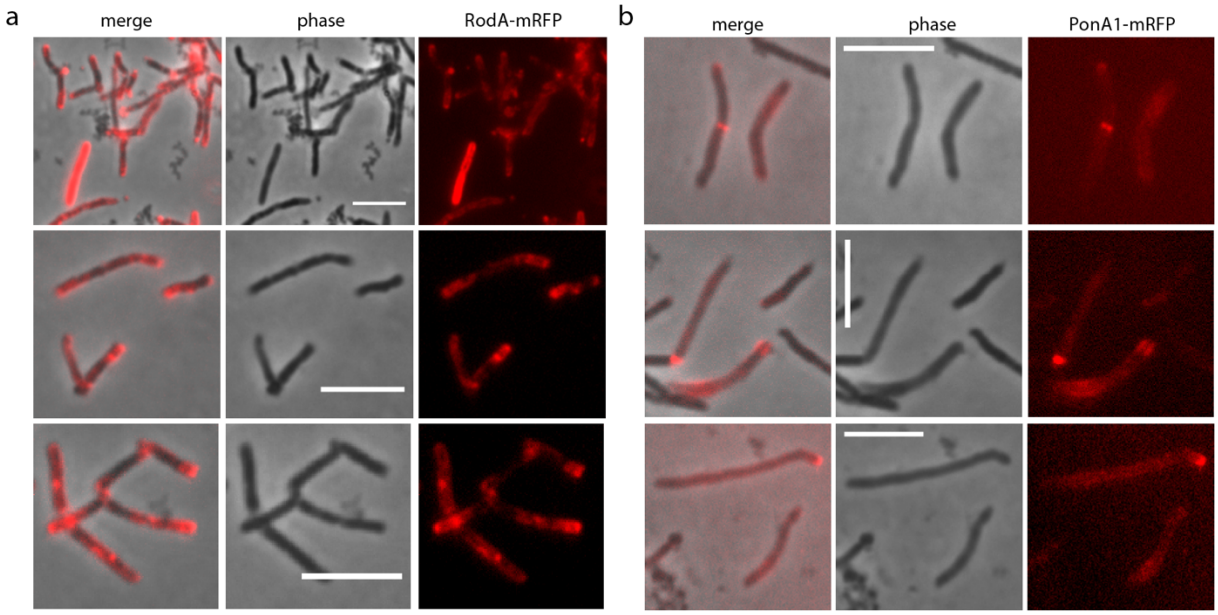

Figure S5: RodA-mRFP and PonA1-mRFP location in cells treated with lysozyme/mutanolysin. Representative images of (a) RodA-mRFP and (b) PonA1-mRFP imaged following mutanolysin/lysozyme treatment. Compare to Figure 1a. Scale bars = 5 μm.

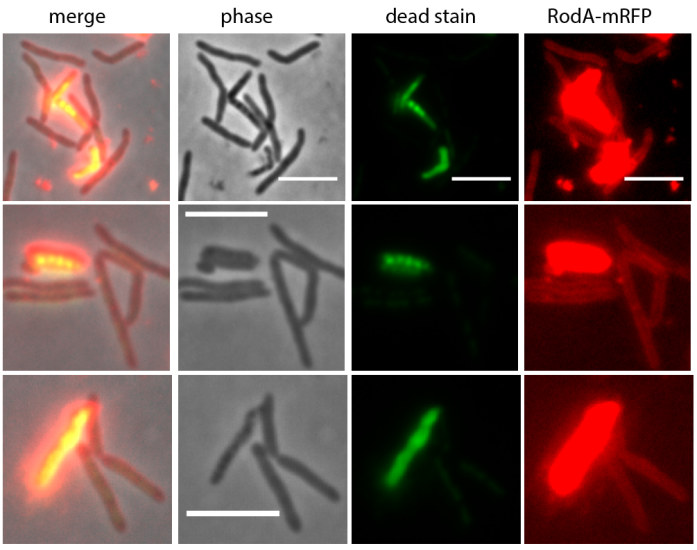

Figure S6: RodA relocalization is not observed in live cells. Staining with dead stain SYTOX green reveals that there are no viable cells that display RodA-mRFP polar relocalization phenotype associated with mutanolysin/lysozyme treatment. Because of spectral crossover of SYTOX Green into the RFP channel in combination with low signal intensity from RodA-mRFP, we were not able to capture RodA-mRFP signal in SYTOX Green-positive cells. Scale bars = 5 μm.

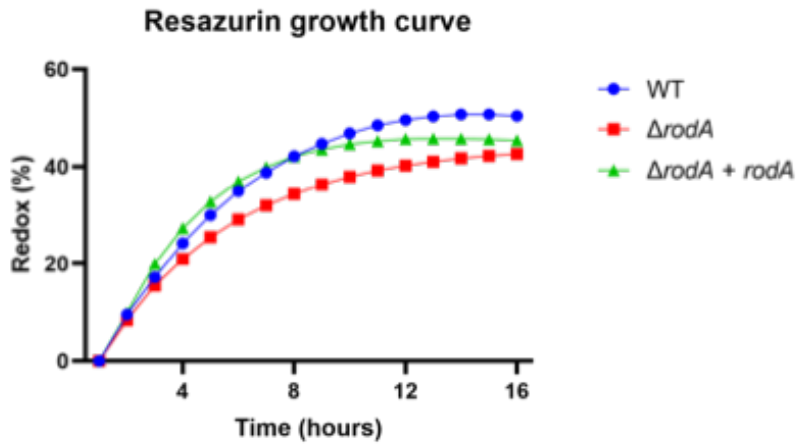

Figure S7: RodA is not required for growth in *M. smegmatis*.

Table S1: Primers used for fluorescent fusion constructs.

gene of interest	primers for *M. smegmatis* gene
rodA-mRFP	TTAATTAAGAAGGAGATATACATatgatgacgacgcaaccccag
	gaCGTCCTCGGAGGAGGCcgagccgcctacctttcgatcacctcgg
lcp1-mRFP	GCTTAATTAAGAAGGAGATATACATatgttgatcaggtccattgctgtg
	CGTCCTCGGAGGAGGCcgagccgccgttcacgcactgcgggtcgttgg
fbpC (MSMEG_3580) -mRFP	CTTAATTAAGAAGGAGATATACATatgcgcggcattgcagcatggaaag
	GTCCTCGGAGGAGGCcgagccgcccgtggcggactgagcgccgagcacc

fbpC	CTTAATTAAGAAGGAGATATACATatgagacgtgggttgagtctggttc
(MSMEG_3580)	
-mRFP	CGTCCTCGGAGGAGGCcgagccgcccttgatggtggcgaccagctcacc
	***mRFP* primers**
	gatcgaaaaggtaggcggctcgGCCTCCTCCGAGGACGtcatca
rodA-mRFP	CCCAATTAATTAGCTAAAGCTTtcaGGCGCCGGTGGAGTGgc
	gatgaCGTCCTCGGAGGAGGCcgagccgccgttcacgcactgcgggtcg
	CCCAATTAATTAGCTAAAGCTTtcaGGCGCCGGTGGAGTGgcggc
lcp1-mRFP	cctc
fbpC	gatgaCGTCCTCGGAGGAGGCcgagccgcccgtggcggactgagcgccg
(MSMEG_3580)	CCCAATTAATTAGCTAAAGCTTtcaGGCGCCGGTGGAGTGgcggc
-mRFP	cctc
fbpC	gatgaCGTCCTCGGAGGAGGCcgagccgcccttgatggtggcgaccagc
(MSMEG_3580)	CCCAATTAATTAGCTAAAGCTTtcaGGCGCCGGTGGAGTGgcggc
-mRFP	cctc

References

1. Paintdakhi A, Parry B, Campos M, Irnov I, Elf J, Surovtsev I, Jacobs-Wagner C. 2016. Oufti: an integrated software package for high-accuracy, high-throughput quantitative microscopy analysis. Mol Microbiol 99:767-77.

2. Garcia-Heredia A, Pohane AA, Melzer ES, Carr CR, Fiolek TJ, Rundell SR, Lim HC, Wagner JC, Morita YS, Swarts BM, Siegrist MS. 2018. Peptidoglycan precursor synthesis along the sidewall of pole-growing mycobacteria. Elife 7.

3. Melzer ES, Sein CE, Chambers JJ, Sloan Siegrist M. 2018. DivIVA concentrates mycobacterial cell envelope assembly for initiation and stabilization of polar growth. Cytoskeleton (Hoboken) 75:498-507.